

RESEARCH ARTICLE

The effect of volume change and stack pressure on solid-state battery cathodes

Boyang Liu^{1,2} | Shengda D. Pu¹ | Christopher Doerrert^{1,2} | Dominic Spencer Jolly¹ | Robert A. House^{1,2} | Dominic L. R. Melvin^{1,2} | Paul Adamson^{1,2} | Patrick S. Grant^{1,2,3} | Xiangwen Gao⁴ | Peter G. Bruce^{1,2,3,5} 

¹Department of Materials, University of Oxford, Oxford, UK

²The Faraday Institution, Didcot, UK

³The Henry Royce Institute, University of Oxford, Oxford, UK

⁴Future Battery Research Center, Global Institute of Future Technology, Shanghai Jiao Tong University, Shanghai, China

⁵Department of Chemistry, University of Oxford, Oxford, UK

Correspondence

Xiangwen Gao, Future Battery Research Center, Global Institute of Future Technology, Shanghai Jiao Tong University, Shanghai, China.
Email: xiangwen.gao@sjtu.edu.cn

Peter G. Bruce, Department of Materials, University of Oxford, Oxford OX1 3PH, UK.
Email: peter.bruce@materials.ox.ac.uk

Funding information

Henry Royce Institute, Grant/Award Numbers: FIRG007, EP/R0066X/1, FIRG008; Engineering and Physical Sciences Research Council, Grant/Award Number: EP/M009521/1; National Natural Science Foundation of China, Grant/Award Number: 22309110

Abstract

Solid-state lithium batteries may provide increased energy density and improved safety compared with Li-ion technology. However, in a solid-state composite cathode, mechanical degradation due to repeated cathode volume changes during cycling may occur, which may be partially mitigated by applying a significant, but often impractical, uniaxial stack pressure. Herein, we compare the behavior of composite electrodes based on $\text{Li}_4\text{Ti}_5\text{O}_{12}$ (LTO) (negligible volume change) and Nb_2O_5 (+4% expansion) cycled at different stack pressures. The initial LTO capacity and retention are not affected by pressure but for Nb_2O_5 , they are significantly lower when a stack pressure of <2 MPa is applied, due to inter-particle cracking and solid-solid contact loss because of cyclic volume changes. This work confirms the importance of cathode mechanical stability and the stack pressures for long-term cyclability for solid-state batteries. This suggests that low volume-change cathode materials or a proper buffer layer are required for solid-state batteries, especially at low stack pressures.

KEYWORDS

cathode, interface, mechanical degradation, stack pressure, solid-state battery

1 | INTRODUCTION

Solid-state batteries employ a solid-state electrolyte (SE) in pursuit of superior safety and to enable the use of a lithium metal anode, which in turn may provide energy densi-

ties that exceed conventional Li-ion batteries (LIB).^{1–3} However, amongst ongoing challenges to developing practical solid-state batteries (SSBs), mechanical and chemical instability at the electrode/SE interface must be overcome for SSBs to realize their full potential.^{4–10} These

This is an open access article under the terms of the [Creative Commons Attribution](https://creativecommons.org/licenses/by/4.0/) License, which permits use, distribution and reproduction in any medium, provided the original work is properly cited.

© 2023 The Authors. *SusMat* published by Sichuan University and John Wiley & Sons Australia, Ltd.

instabilities occur in the solid-state composite cathode (SSC), which is composed of a particulate mixture of the cathode active material (CAM), the SE, and generally carbon additives.

Oxides and sulfides are two of the most well-studied groups of SE. Oxide-type SEs have advantages including high mechanical strength, high temperature tolerance, stability against air and solvents, and wide electrochemical stable window.¹¹ However, the rigid oxide-based SE could not form a good connection between particles and grains without high-temperature sintering. The high-temperature sintering will cause undesired elemental diffusion between the CAM and oxides.^{12–14} Therefore, it is challenging to form a direct cathode/oxide SE particle contact for most types of cathodes. Different from oxides, sulfide-based SEs have high ionic conductivities and deformability at low/intermediate temperatures, desirable for processing electrodes to high, near theoretical density.^{15–20} However, sulfides are susceptible to oxidation at the operating potentials required for the CAM (such as $\text{Li}(\text{Ni}_x\text{Co}_y\text{Mn}_{1-x-y})\text{O}_2$ and $\text{Li}(\text{Ni}_x\text{Co}_y\text{Al}_{1-x-y})\text{O}_2$).^{21–23} Even when CAM particles are coated with a protective layer (e.g., oxide) that partially passivates the surface, carbon additives required for electron percolation, such as carbon nanofiber (CNF), may also play a role in oxidizing the sulfide electrolyte.^{24,25} In both cases, ongoing chemical interaction undermines retained capacity and cyclability. Mechanically, the cyclic volume change of the CAM during the induced insertion/extraction of Li-ion can lead to sudden or progressive contact loss between the sulfide SE, CNF, and CAM, resulting in voiding and irreversible loss of capacity.^{26–30} Cracking of CAM particles themselves may also occur.^{31–34} To mitigate some of the mechanical effects (and ongoing porosity due to sub-optimal electrode preparation), cells may be subject to a relatively high uniaxial stack pressure of over 50 MPa during cyclic testing. However, a much lower stack pressure is required for practical applications, for example, in electric vehicles,^{35,36} and excessive pressure may accelerate the damage of CAM particles and lead to the deformation of Li metal electrodes. Given this complexity and interaction of SSC capacity fading mechanisms, separation of mechanical degradation from chemical and electrochemical side reactions is vital to elucidating the various processes occurring and searching for corresponding strategies.

Here, we investigate the effects of CAM volume change and stack pressure on the capacity decay of SSCs. Two model active materials with the same voltage window but different volume changes during cycling were chosen, including $\text{Li}_4\text{Ti}_5\text{O}_{12}$ (LTO) with a negligible volume change and $\alpha\text{-Nb}_2\text{O}_5$ with 4% expansion on Li intercalation^{37,38} to compare the effects of intrinsic volume changes on retained capacity. Each CAM is combined

with $\text{Li}_6\text{PS}_5\text{Cl}$ (LPSC) as the SE and CNF additive to form the SSC and a potential range of 1.4–1.9 V versus Li^+/Li was chosen, where LPSC does not exhibit significant electrochemical degradation.^{39,40} Therefore, the mechanical degradation effect can be decoupled from the chemical reactivity. We find that LTO can be stably cycled at pressures as low as 0.1 MPa, which is a reasonable pressure for practical pouch cell applications without external pressure configurations, while significant fading was observed for Nb_2O_5 at low stack pressures due to contact loss. Voids form inside the cathode, which severely reduces the capacity retention. A zero-strain cathode or a buffer layer is therefore required to achieve sustained cycling for SSCs at low stack pressures.

2 | RESULTS AND DISCUSSION

Nb_2O_5 and LTO were incorporated into SSCs with LPSC and CNF at a volume ratio of 10:10:1, as described in the Supporting Information. As shown in the scanning electron microscope (SEM) images in Figure S1, the particle sizes of Nb_2O_5 and LTO were comparable. The electrochemical stability of LPSC between 1.4 and 1.9 V was investigated by galvanostatic cycling of an SSC composed of LPSC and CNF. The specific capacity was close to 0 mAhg^{-1} , indicating that no significant degradation of LPSC occurs in this voltage range. The X-ray photoelectron spectra (XPS) before and after 100 cycles in Figure S2 showed no new compounds were generated during cycling, further confirming the stability of LPSC, in agreement with previous reports.^{39,40}

In order to avoid the effect of the counter electrode and focus on the investigation of the working electrode, a custom-designed three-electrode cell was utilized with the LTO/LPSC or Nb_2O_5 /LPSC composite as the working electrode, prelithiated LTO/LPSC composite as the counter electrode and Li metal as the reference electrode, with further details in the Supporting Information. Prelithiated LTO was selected as the counter electrode because it had a constant volume during cycling and provided negligible stress against the working electrode. Electrochemical cycling was carried out at 60°C to promote ion mobility and to ensure high utilization of the CAM. The ionic conductivity of LPSC at 60°C increased from 5.3 to $7.7 \times 10^{-3} \text{ S/cm}$ between 0.1 and 50 MPa (Figure S1D,E). The apparent conductivity increased with higher stack pressure because of the better contact between LPSC and the current collector surface. The same trend was reported at room temperature previously.⁴¹ Although the ionic conductivity of LPSC changed with stack pressure, even at 0.1 MPa stack pressure, it is still high enough for the full utilization of the CAM for the selected electrode loading and rate.⁴²

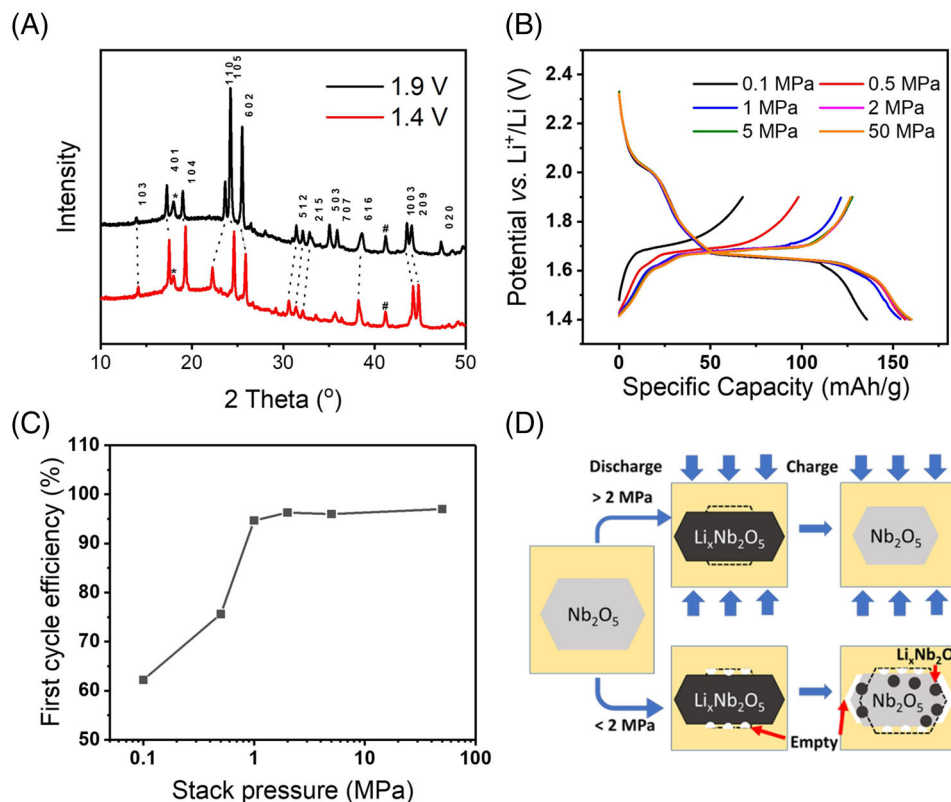


FIGURE 1 Electrochemical behavior of the Nb₂O₅/LPSC composite electrode under different stack pressures. (A). In-situ X-ray diffraction (XRD) of Nb₂O₅ at different stages of lithiation (1.9 and 1.4 V vs. Li⁺/Li). The peaks marked with * are from the PTFE inside the electrode. (B) 1st cycle voltage profiles and (C) Coulombic efficiency of the composite electrode under various stack pressures. The efficiency is defined as the ratio of total charge capacity and the discharge capacity between 1.4 and 1.9 V. (D) Schematic of the Nb₂O₅/LPSC particle interface over the 1st cycle under high and low stack pressures.

Figure 1 shows the relation between the 1st cycle of Nb₂O₅/LPSC composite electrodes and the stack pressures. Nb₂O₅ was pre-treated to achieve the α phase with the details in the Supporting Information, which is confirmed by the X-ray diffraction (XRD) shown in Figure S3. The in-situ XRD profiles from Nb₂O₅ over discharge were tested to calculate the volume change of the Nb₂O₅ (Figure 1A). Based on lattice parameters matching and calculation, the volume expansion was 3.8% and was anisotropy (Table S1). The volume expansion was lower than the 6% reported in literature^{37,38} because the Nb₂O₅ in this work was not fully lithiated in our selected voltage window. The 1st cycle voltage profiles of the Nb₂O₅/LPSC composite electrode at various stack pressures are shown in Figure 1B. Compared with the discharge capacities, the loss of charge capacities at low pressures was more severe. For cells discharged at stack pressures ≥ 0.5 MPa, the 1st discharge capacities were ~ 156 mAh/g, while for cells at 0.1 MPa, the capacity was reduced to 135 mAh/g. In the 1st charging process, the cells with ≥ 2 MPa stack pressures had similar capacities of 127 mAh/g, while cells at 1, 0.5, and 0.1 MPa had reduced capacities of 121, 98, and 65 mAh/g, respectively.

Figure 1C shows the first cycle Coulombic efficiency of the Nb₂O₅/LPSC cathode at different stack pressures, which is defined as the percentage of discharge capacity recovered on charging on cycling between 1.4 and 1.9 V. The efficiency was over 95% for stack pressures ≥ 1 MPa but reduced to only 62% at 0.1 MPa. The high stack pressure can hold the Nb₂O₅/LPSC contact during charge and discharge, while at a lower stack pressure, the contact was reduced due to the volume change of Nb₂O₅. This resulted in the porous interface, void formation, and incomplete delithiation in the Nb₂O₅ particles (Figure 1D).

In contrast to Nb₂O₅ with 3.8 % volume change, LTO, which has similar working potentials but no volume change over lithiation, showed an approximately constant charge capacity of 154 mAh/g (Figure 2A) and a 1st cycle Coulombic efficiency of approximately 98% (Figure 2B) at stack pressures ranging from 0.1 to 50 MPa. The role of stack pressure is to maintain the micro-scale integrity and physical contact of a high fraction of SE/CAM particle interfaces, where otherwise expansion or contraction of the CAM would lead to debonding and/or cracking, and ionic or electronic isolation of the CAM. The stable LTO

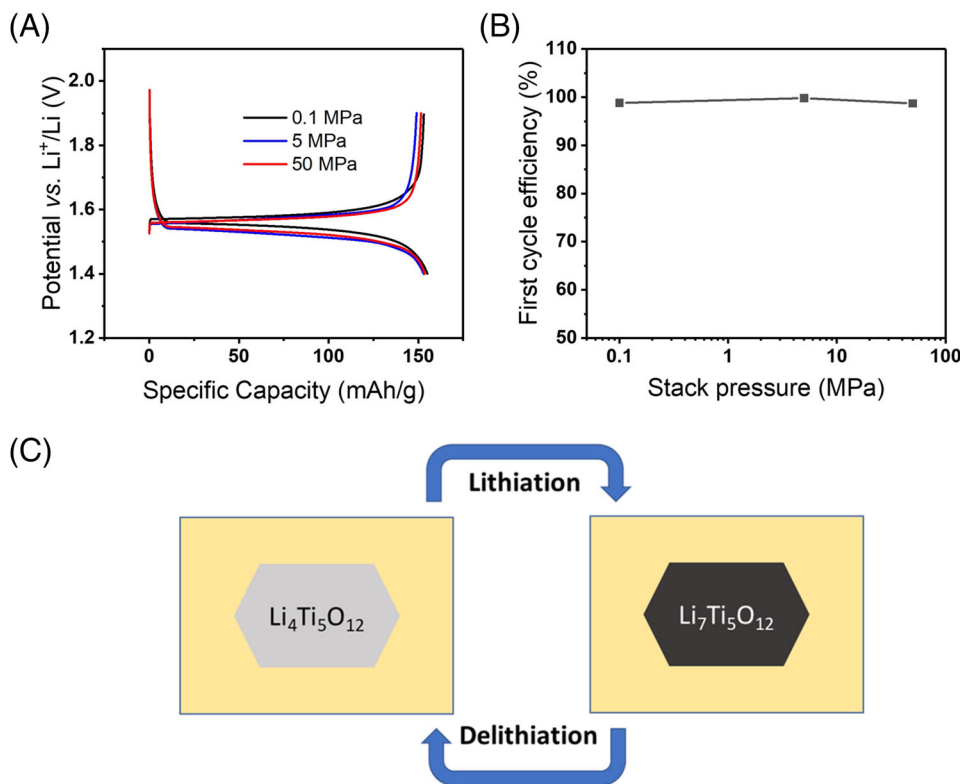


FIGURE 2 Electrochemical behavior of the $\text{Li}_4\text{Ti}_5\text{O}_{12}/\text{Li}_6\text{PS}_3\text{Cl}$ (LTO/LPSC) composite electrode at different stack pressures. (A) 1st cycle voltage profiles and (B) Coulombic efficiency of the composite electrode under various stack pressures. The efficiency is defined as the ratio of total charge capacity and the discharge capacity between 1.4 and 1.9 V. (C) Schematic of the LTO/LPSC particle interface over the 1st cycle. The particle interface was stable regardless of stack pressures.

particles protect the CAM/SE interface from delamination and ensure good contact during charge and discharge, even without external pressures, as illustrated in Figure 2C.

The cyclability of Nb_2O_5 -based composite electrodes at different stack pressures is shown in Figure 3A. The voltage profiles of the 1st and 30th cycles are shown in Figure 3B,C. At stack pressures between 2 and 50 MPa, the charge capacity retention was constant at 96 % over 30 cycles. However, at lower stack pressures of 0.1–1 MPa, the capacity retention was much reduced. This difference suggested that a stack pressure ≥ 2 MPa was required to maintain an intimate CAM/SE interface during cycling. For the cell cycled at 0.1 MPa, the Coulombic efficiency was 90% in the 2nd cycle and gradually increased to 98% in the following cycles, while for the cell cycling under a higher stack pressure, the Coulombic efficiency was already over 98% from the 2nd cycle (Figure S14A). The XPS profiles of LPSC in the SSC before and after 30 cycles (Figure S5) confirmed the chemical and electrochemical stability of the $\text{Nb}_2\text{O}_5/\text{LPSC}$ interface within the voltage range used. Therefore, the capacity decay under low stack pressures for the Nb_2O_5 -based SSC may be ascribed principally to the mechanical degradation. The efficiency of the cell at 0.1 MPa after the 2nd cycle ($>90\%$) was much higher than

the 1st cycle (62%), indicating that the most severe mechanical degradation happened in the 1st cycle and it became slower from the 2nd cycle. To investigate the microstructural changes in the SSC, cross-sectional SEM images of the $\text{Nb}_2\text{O}_5/\text{LPSC}$ composites before and after cycling are shown in Figure 3B–D where cross-sections were prepared by plasma focused-ion beam (P-FIB). The CAM and LPSC were differentiated as the lighter and darker grayscale in the images respectively, with black areas representing voids. The upright curtain-shaped lines in the FIB-SEM images were formed by the ion beam for milling. This is due to the soft nature of LPSC, and the lowest limitation of ion beam current. The bright dots were because of the remaining high temperature on the particles after milled by the ions.

Before cycling, the pristine SSC in Figure 3D shows that Nb_2O_5 and LPSC particles formed continuous physical contact throughout. The composite electrode cycled at 0.5 MPa developed significant voiding from inter-particle cracking, which is marked as the dashed lines in Figure 3E, whereas the electrode cycled at 5 MPa maintained a much higher fraction of contacting interfaces and comparatively low incidences of cracking (Figure 3F). The different morphologies shown by the FIB-SEM are in accord with the

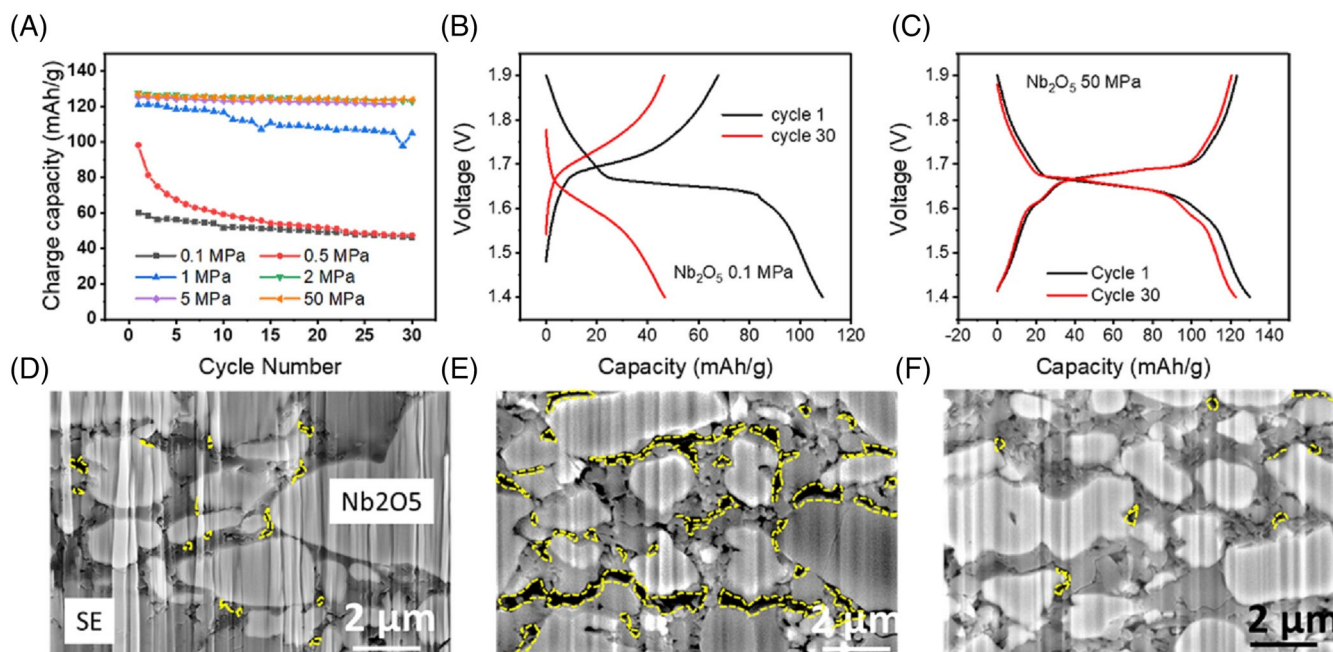


FIGURE 3 Cycling behaviors and scanning electron microscope (SEM) before and after cycling of Nb₂O₅ solid-state composite cathode (SSC). (A) Cycling behaviors of Nb₂O₅ at different stack pressures. (B, C) Voltage profiles of the Nb₂O₅ on 1st and 30th cycles at 0.1 (B) and 50 (C) MPa stack pressures. (D–F) Cross-sectional SEM of the SSCs before and after cycling: (D) Pristine Nb₂O₅/LPSC cathode. (E) Nb₂O₅/LPSC cathode after 30 cycles at 0.5 MPa. (F) Nb₂O₅/LPSC cathode after 30 cycles at 5 MPa. In Figure D–F, the cracking/empty space between particles was marked by yellow dashed lines.

low coulombic efficiency and poor capacity retention at lower stack pressures and suggest a stack pressure of no less than 2 MPa is needed to maintain an intimate and effective interface between Nb₂O₅ and LPSC during cycling.

In comparison, the LTO/LPSC SSC had a stable capacity retention of 100% over 30 cycles even at a low stack pressure of 0.1 MPa (Figure 4A), and the Coulombic efficiency maintained > 99% over many cycles under different stack pressures, as shown in Supporting Information Figure S14b. The voltage profiles of the 1st and 30th cycles of LTO at 0.1 MPa are shown in Figure 4B. Figure 4C,D shows the cross-sectional SEM images of LTO/LPSC SSC before and after 30 cycles at 0.1 MPa. The microstructure is minimal changed, with no clear evidence of cracking after cycling. A comparison of the post-cycle morphologies of the SSC with Nb₂O₅ and LTO indicated that the SE/CAM interface delamination was caused mainly by the CAM volume change, especially at a low stack pressure. The results suggest that whole capacity degradation by interfacial debonding and cracking can be partially mitigated by stack pressures, and intrinsically low-volume change materials provide a distinct advantage at low pressures.

This work indicated that the critical stack pressure is related to the volume change ratio of the active material. Here, we compared LTO with 0 strain and Nb₂O₅ with 4% expansion. Other works reported that for large-

volume changing electrode material like Silicon, a much higher stack pressure of 50–120 MPa was used for stable cycling.^{43,44} Therefore, the volume change ratio is a determining factor of the stack pressure. The elasticity of the SE would also affect the cycling stability of the composite electrode. Lower mechanical strength of the electrolyte results in less contact loss and higher stability.⁴⁵ It was also predicted by modeling that a lower stiffness SE has a better tolerance of the active materials volume change.⁴⁶ However, the applied stack pressure in these works was not carefully controlled and reported in the mentioned works. The active material mechanical modulus' effect on the critical stack pressure is not clear yet, because the different cathode materials have different specific capacity and volume expansion ratios and are hard to compare and find the effect of the different modulus. The critical stack pressure could also be affected by other variables, including the particle sizes and conductivities of active material and solid electrolytes, the thickness of the cathode layer, and the uniformity and densification of the composite electrode. The quantitative description is still an open question to solve.

In conclusion, the mechanical stability of two model composite cathodes with 4% volume change (Nb₂O₅) and with negligible volume change (LTO) has allowed the decoupling of the chemical and mechanical contributions to capacity degradation in solid-state battery cathodes. Cells cycled at various stack pressures showed that the

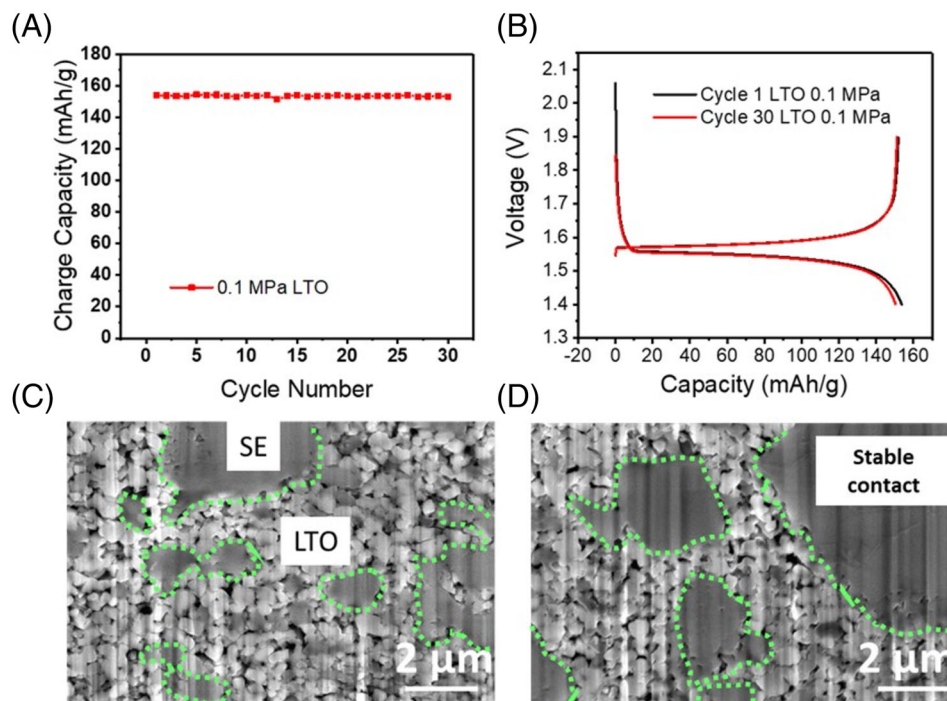


FIGURE 4 Cycling behavior and scanning electron microscope (SEM) before and after cycling of $\text{Li}_4\text{Ti}_5\text{O}_{12}$ (LTO) solid-state composite cathode (SSC). (A) Cycling behavior of LTO at 0.1 MPa stack pressure. (B) Voltage profiles of the LTO in the 1st and 30th cycles at 0.1 MPa stack pressure. (C, D). Cross-sectional SEM of the SSCs before and after 30 cycles at 0.1 MPa: (C) Pristine LTO SSC. (D) LTO SSC after 30 cycles at 0.1 MPa. The interface between LTO and SE was marked with green dashed lines.

first-cycle efficiency and capacity retention ratio over cycling of Nb_2O_5 were reduced at a stack pressure of less than 2 MPa, while LTO maintained almost 100% first-cycle efficiency and capacity retention even at a low stack pressure of 0.1 MPa. Volume changes of the CAM caused CAM/SE microscopic interfacial delamination, which could be prevented by applying high stack pressures or substituting with an intrinsically low volume change CAM. This work has helped to clarify the relationship between cathode volume change, stack pressure, and capacity retention. These conclusions bring to the forefront the interesting materials discovery challenge for identifying new cathode materials with both high energy density and low volume change ratio for realistic solid-state batteries.

ACKNOWLEDGMENTS

Peter G. Bruce is indebted to the Henry Royce Institute SOLBAT (FIRG007 and FIRG008), as well as the Engineering and Physical Sciences Research Council, Enabling Next Generation Lithium Batteries (EP/M009521/1), and the Henry Royce Institute for Advanced Materials (EP/R0066X/1, EP/S019367/1, and EP/R010145/1) for financial support. Xiangwen Gao acknowledges financial support from the National Natural Science Foundation of China (22309110).

CONFLICT OF INTEREST STATEMENT

The authors declare no conflict of interest.

ORCID

Peter G. Bruce  <https://orcid.org/0000-0001-6748-3084>

REFERENCES

1. Famprikis T, Canepa P, Dawson JA, Islam MS, Masquelier C. Fundamentals of inorganic solid-state electrolytes for batteries. *Nat Mater*. 2019;18(12):1278-1291.
2. Zhao Q, Stalin S, Zhao CZ, Archer LA. Designing solid-state electrolytes for safe, energy-dense batteries. *Nat Rev Mater*. 2020;5(3):229-252.
3. Zaman W, Hatzell KB. Processing and manufacturing of next generation lithium-based all solid-state batteries. *Curr Opin Solid State Mater Sci*. 2022;26(4):101003.
4. Li Y, Zhang D, Xu X, et al. Interface engineering for composite cathodes in sulfide-based all-solid-state lithium batteries. *J Energy Chem*. 2021;60:32-60.
5. Vishnugopi BS, Kazyak E, Lewis JA, et al. Challenges and opportunities for fast charging of solid-state lithium metal batteries. *ACS Energy Lett*. 2021;6(10):3734-3749.
6. Nie K, Hong Y, Qiu J, et al. Interfaces between cathode and electrolyte in solid state lithium batteries: challenges and perspectives. *Front Chem*. 2018;6:616.
7. Xiang Y, Li X, Cheng Y, Sun X, Yang Y. Advanced characterization techniques for solid state lithium battery research. *Mater Today*. 2020;36:139-157.

8. Garcia-Mendez R, Smith JG, Neufeind JC, Siegel DJ, Sakamoto J. Solid-state batteries: correlating macro and atomic structure with elastic properties and ionic transport of glassy Li₂S-P₂S₅ (LPS) solid electrolyte for solid-state Li metal batteries. *Adv Energy Mater.* 2020;10(19):2070085.
9. Ren Y, Hortance N, Hatzell KB. Mitigating chemo-mechanical failure in Li-S solid state batteries with compliant cathodes. *J Electrochem Soc.* 2022;169(6):060503.
10. Yu HC, Taha D, Thompson T, et al. Deformation and stresses in solid-state composite battery cathodes. *J Power Sources.* 2019;440:227116.
11. Kim A, Woo S, Kang M, Park H, Kang B. Research progresses of garnet-type solid electrolytes for developing all-solid-state Li batteries. *Front Chem.* 2020;8:468.
12. Roitzheim C, Sohn YJ, Kuo L-Y, et al. All-solid-state Li batteries with NCM-garnet-based composite cathodes: the impact of NCM composition on material compatibility. *ACS Appl Energy Mater.* 2022;5(6):6913-6926.
13. Park K, Yu B-C, Jung J-W, et al. Electrochemical nature of the cathode interface for a solid-state lithium-ion battery: interface between LiCoO₂ and garnet-Li₇La₃Zr₂O₁₂. *Chem Mater.* 2016;28(21):8051-8059.
14. Ihrig M, Finsterbusch M, Laptev AM, et al. Study of LiCoO₂/Li₇La₃Zr₂O₁₂:ta interface degradation in all-solid-state lithium batteries. *ACS Appl Mater Interfaces.* 2022;14(9):11288-11299.
15. Wang C, Liang J, Zhao Y, Zheng M, Li X, Sun X. All-solid-state lithium batteries enabled by sulfide electrolytes: from fundamental research to practical engineering design. *Energy Environ Sci.* 2021;14(5):2577-2619.
16. Yu T, Ke B, Li H, Guo S, Zhou H. Recent advances in sulfide electrolytes toward high specific energy solid-state lithium batteries. *Mater Chem Front.* 2021;5(13):4892-4911.
17. Umeshbabu E, Zheng B, Yang Y. Recent progress in all-solid-state lithium-sulfur batteries using high Li-ion conductive solid electrolytes. *Energy Rev.* 2019;2:129-230.
18. Zhou L, Minafra N, Zeier WG, Nazar LF. Innovative approaches to Li-argyrodite solid electrolytes for all-solid-state lithium batteries. *Acc Chem Res.* 2021;54(12):2717-2728.
19. Zhou L, Assoud A, Zhang Q, Wu X, Nazar LF. New family of argyrodite thioantimonate lithium superionic conductors. *J Am Chem Soc.* 2019;141(48):19002-19013.
20. Doerr C, Capone I, Narayanan S, et al. High energy density single-crystal NMC/Li₆PS₅Cl cathodes for all-solid-state lithium-metal batteries. *ACS Appl Mater Interfaces.* 2021;13(31):37809-37815.
21. Jung SK, Gwon H, Lee SS, et al. Understanding the effects of chemical reactions at the cathode-electrolyte interface in sulfide based all-solid-state batteries. *J Mater Chem A.* 2019;7(40):22967-22976.
22. Brahmabhatt T, Yang G, Self E, Nanda J. Cathode-sulfide solid electrolyte interfacial instability: challenges and solutions. *Front Energy Res.* 2020;8(October):1-10.
23. Byeon Y-W. Review on interface and interphase issues in sulfide solid-state electrolytes for all-solid-state Li-metal batteries. *Electrochem.* 2021;2(3):452-471.
24. Auvergniot J, Cassel A, Ledeuil J, Viallet V, Seznec V, Dedryvère R. Interface stability of argyrodite Li₆PS₅Cl toward LiCoO₂, LiNi_{1/3}Co_{1/3}Mn_{1/3}O₂, and LiMn₂O₄ in bulk all-solid-state batteries. *Chem Mater.* 2017;29(9):3883-3890.
25. Dewald GF, Ohno S, Kraft MA, et al. Experimental assessment of the practical oxidative stability of lithium thiophosphate solid electrolytes. *Chem Mater.* 2019;31(20):8328-8337.
26. Zhang F, Huang QA, Tang Z, et al. A review of mechanics-related material damages in all-solid-state batteries: mechanisms, performance impacts and mitigation strategies. *Nano Energy.* 2020;70:104545.
27. Conforto G, Ruess R, Schröder D, et al. Quantification of the impact of chemo-mechanical degradation on the performance and cycling stability of NCM-based cathodes in solid-state Li-ion batteries. *J Electrochem Soc.* 2021;168(7):070546.
28. Koerver R, Zhang W, Biasi LDe, et al. Chemo-mechanical expansion of lithium electrode materials – on the route to mechanically optimized all-solid-state batteries. *Energy Environ Sci.* 2018;11(8):2142-2158.
29. Lee E, Kwon BJ, Dogan F, Ren Y, Croy JR, Thackeray MM. Lithiated spinel LiCo_{1-x}Al_xO₂ as a stable zero-strain cathode. *ACS Appl Energy Mater.* 2019;2(9):6170-6175.
30. Strauss F, de Biasi L, Kim A-Y, et al. Rational design of quasi-zero-strain NCM cathode materials for minimizing volume change effects in all-solid-state batteries. *ACS Mater Lett.* 2020;2(1):84-88.
31. Koerver R, Aygu I, Leichtweiß T, et al. Capacity fade in solid-state batteries: interphase formation and chemomechanical processes in nickel-rich layered oxide cathodes and lithium thiophosphate solid electrolytes. *Chem Mater.* 2017;29(13):5574-5582.
32. Shi T, Zhang Y, Tu Q, Wang Y, Scott MC, Ceder G. Characterization of mechanical degradation in an all-solid-state battery cathode. *J Mater Chem A.* 2020;8(34):17399-17404.
33. Koerver R, Zhang W, De Biasi L, et al. Chemo-mechanical expansion of lithium electrode materials-on the route to mechanically optimized all-solid-state batteries. *Energy Environ Sci.* 2018;11(8):2142-2158.
34. Han Y, Jung SH, Kwak H, et al. Single- or poly-crystalline Ni-rich layered cathode, sulfide or halide solid electrolyte: which will be the winners for all-solid-state batteries? *Adv Energy Mater.* 2021;11(21):2100126.
35. Albertus P, Anandan V, Ban C, et al. Challenges for and pathways toward Li-metal-based all-solid-state batteries. *ACS Energy Lett.* 2021;6(4):1399-1404.
36. Chen R, Li Q, Yu X, Chen L, Li H. Approaching practically accessible solid-state batteries: stability issues related to solid electrolytes and interfaces. *Chem Rev.* 2020;120(14):6820-6877.
37. Catti M, Ghaani MR. On the lithiation reaction of niobium oxide: structural and electronic properties of Li_{1.714}Nb₂O₅ michele. *Phys Chem Chem Phys.* 2014;16(4):1385-1392.
38. Song Z, Li H, Liu W, et al. Ultrafast and stable Li- (De) intercalation in a large single crystal H-Nb₂O₅ anode via optimizing the homogeneity of electron and ion transport. *Adv Mater.* 2020;32(22):2001001.
39. Tan DHS, Wu EA, Nguyen H, et al. Elucidating reversible electrochemical redox of Li₆PS₅Cl solid electrolyte. *ACS Energy Lett.* 2019(10):2418-2427.
40. Schwieter TK, Arszewska VA, Wang C, et al. Clarifying the relationship between redox activity and electrochemical stability in solid electrolytes. *Nat Mater.* 2020;19(4):428-435.

41. Doux J, Yang Y, Tan DHS, et al. Pressure effects on sulfide electrolytes for all solid-state batteries. *J Mater Chem A*. 2020;8(10): 5049-5055.
42. Bielefeld A, Weber DA, Janek J. Modeling effective ionic conductivity and binder influence in composite cathodes for all-solid-state batteries. *ACS Appl Mater Interfaces*. 2020;12(11):12821-12833.
43. Sakabe J, Ohta N, Ohnishi T, Mitsuishi K, Takada K. Porous amorphous silicon film anodes for high-capacity and stable all-solid-state lithium batteries. *Commun Chem*. 2018;1(1): 24.
44. Tan DHS, Chen Y-T, Yang H, et al. Carbon-free high-loading silicon anodes enabled by sulfide solid electrolytes. *Science (80-)*. 2021;373(6562):1494-1499.
45. Kato A, Yamamoto M, Sakuda A, Hayashi A, Tatsumisago M. Mechanical properties of $\text{Li}_2\text{S}-\text{P}_2\text{S}_5$ glasses with lithium halides and application in all-solid-state batteries. *ACS Appl Energy Mater*. 2018;1(3):1002-1007.
46. Bucci G, Swamy T, Chiang Y, Carter WC. Modeling of internal mechanical failure of all-solid-state batteries during electrochemical cycling, and implications for battery design. *J Mater Chem A*. 2017;5(36):19422-19430.

SUPPORTING INFORMATION

Additional supporting information can be found online in the Supporting Information section at the end of this article.

How to cite this article: Liu B, Pu SD, Doerr C, et al. The effect of volume change and stack pressure on solid-state battery cathodes. *SusMat*. 2023;3:721–728. <https://doi.org/10.1002/sus2.162>